Flow and Thermal Transport Studies in Microchannel Flows using Lattice Boltzmann Method

Rajlakshmi Nayak, Savithiri. S, Dhiman Chatterjee and Sarit K. Das[1]
Department of Mechanical Engineering,
Indian Institute of Technology Madras, Chennai-36, India

ABSTRACT
The present study numerically investigates the hydrodynamic and thermal characteristics of single phase pressure driven flow for a single square microchannels using Lattice Boltzmann method (LBM). Two dimensional and nine directional model (D_2Q_9) in Lattice Boltzmann method is used to simulate the flow and water is considered as the working fluid. Uniform temperature is assumed at the channel walls and the fluid temperature is taken to be lower than that of the wall. Hydrodynamic and thermal entrance lengths are determined using Lattice Boltzmann method for different Reynolds numbers (5, 10, 50 and 100). The results obtained are compared with the available experimental μ-PIV studies and thermal studies in literature and found to be consistent.

1. INTRODUCTION

Microchannel flows have got significant relevance in both natural and artificial systems. The surface (transport) to volume (bulk motion) ratio increases with decrease in hydraulic diameter. Hence, with the decrease in hydraulic diameter we can achieve better transport. In many applications involving microchannels, the channel length is kept low because of very high pressure drop. Since the channel lengths are small the transport characteristics are influenced by the entrance length, demanding the need for study in the developing flow region.

A number of hydrodynamic entrance length studies were carried out both experimentally and numerically [1–3]. Thermal entrance length problems are mostly solved by assuming hydrodynamically developed flow at entrance. Wibulswas [4] studied flow characteristics microchannels with the circumferential constant wall temperature and axial constant wall heat flux boundary conditions. Aparecido and Cotta [5] found analytical solutions for square ducts for the uniform wall temperature boundary conditions, both axially and circumferentially. Ahmad and Hassan [6] reported hydrodynamic entrance length in a square microchannel with the help of μ-PIV over a range of Reynolds number from 0.5 to 200 and proposed correlations for the hydrodynamic entrance length for the diameter below 200 mm. Lee *et al.*[7] reported both experimentally and computationally the thermally developing flow and heat transfer studies in microchannels with various aspect ratios. They suggested correlation for Nusselt number as a function of aspect ratio and the effect of entrance length on heat transfer. Although earlier experimental and numerical studies are available, this study is a new approach that resolves the flow and thermal characteristics in a microchannel by Lattice Boltzmann method (LBM). LBM, a particle-based approach has received considerable attention for simulation of viscous flows. Unlike the traditional computation fluid dynamics (CFD), which numerically solves the conservation equations of macroscopic properties (i.e., mass, momentum, and energy), LBM models the fluid consisting of fictitious particles, and such particles perform consecutive propagation and collision processes over a discrete lattice mesh. Due to its particulate nature and local dynamics, LBM has several advantages over conventional CFD methods, viz., reduction from second-order to first-order partial differential equations, simplification of nonlinear modeling, computational efficiency and

[1]Corresponding author: skds@iitm.ac.in

accuracy, simple fluid interface boundary conditions and a mathematical frame-work allowing molecular level modeling. Therefore, it is effective for problems in which both mesoscopic and microscopic statistics become important, as in the case of microchannels [8]. Most of the literature have reported studies on air flow in microchannels [9–11].

The present numerical study analyses the hydrodynamic and thermal characteristics of water flowing in a square microchannel using an in-house LBM code. This study focuses on the effect of Reynolds number on hydrodynamic and thermal entrance lengths for a microchannel flow with uniform wall temperature boundary condition.

2. COMPUTATIONAL STUDY USING LBM

2.1. Geometry and computational domain

The present numerical study analyses the hydrodynamic and thermal characteristics of water flowing in a square microchannel as shown in Figure 1(a). The aspect ratio (L/H) of the two dimensional computational domain is taken as 10 in order to get fully developed flow at outlet of the channel. The flow is assumed to be steady, incompressible, laminar and with constant fluid properties. The viscous dissipation effects are neglected in the present study. A two dimensional rectangular computational domain as shown in Figure 1(b) is considered for the study. It consists of two dimensional spatial lattices of dimensions nx × ny.

A uniform velocity (u_i) profile is defined at the inlet and pressure outlet boundary condition is defined at the exit. No slip conditions are assumed at the channel walls. Uniform temperature (T_{wall}) is assumed at the channel walls and the fluid temperature is taken to be lower than that of the wall.

2.2. Governing equations and boundary conditions

Conservation of mass: $$\frac{\partial \rho}{\partial t} + \nabla \cdot (\rho u) = 0 \quad (1)$$

Conservation of momentum: $$\frac{\partial u}{\partial t} + (u \cdot \nabla) u = -\frac{1}{\rho} \nabla p + \nu \nabla^2 u \quad (2)$$

Conservation of energy: $$\left(\rho C_p\right)\left[\frac{\partial T}{\partial t} + u \cdot \nabla T\right] = \nabla \cdot k \nabla T \quad (3)$$

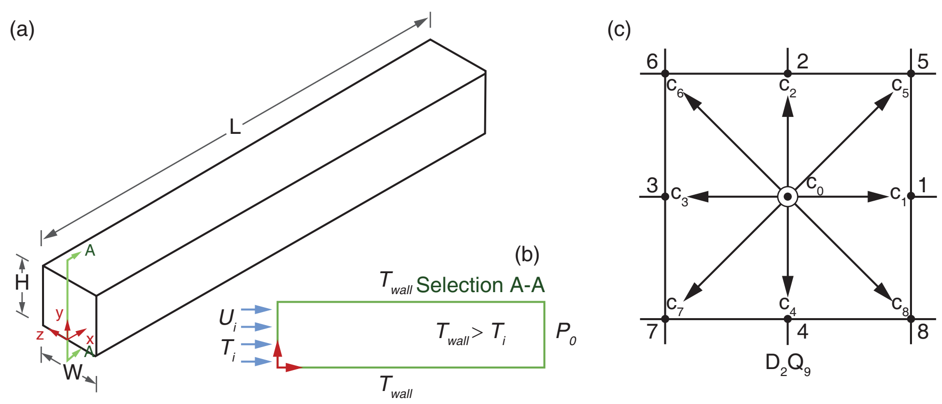

Figure 1. (a) Schematic of microchannel geometry (b) Computational domain for present study (c) D_2Q_9 Lattice arrangement

The boundary conditions are given as follow

at $x = 0$ and $0 \le y \le H$; $T = T_c$, $u = u_i$, $v = 0$ (4a)

at $x = L$ and $0 \le y \le H$; $p = 1$ (4b)

at $y = 0, H$ and $0 \le x \le L$; $T = T_{wall}$ (4c)

The local variation of Nusselt number in the channel can be expressed as $Nu_x = -\frac{\partial \theta}{\partial y}$

In the channel wall average Nusselt number is an integration of local Nusselt number over the length (L) of the channel

$$Nu_{avg} = \int_0^1 Nu_x \, dx \qquad \text{where, } \theta = \frac{(T - T_c)}{(T_h - T_c)} \tag{5}$$

The simple bounce back scheme for no slip velocity condition is applied to all the channel walls. The temperature boundary conditions are defined by specifying non-dimensional temperature which is 0 at the channel inlet and 1 at the hot channel walls.

2.3. LBM algorithm

In LBM, a fluid is modeled as fictitious particles moving in a lattice domain at discrete time steps. The major variable in LBM is the density distribution $f_i\,(x, t)$, indicating the number of particles moving along the i^{th} lattice direction at position x and time t. The basic algorithm of LBM has two processes, collision and streaming. To solve the flow and temperature, two Lattice Boltzmann equations for BGK approximation [3, 13] is written as

$$f_i(x + c_i t, t + \Delta t) = -\frac{f_i(x,t) - f_i^{eq}(x,t)}{\tau_{mom}} \tag{6}$$

$$g_i(x + c_i t, t + \Delta t) = -\frac{g_i(x,t) - g_i^{eq}(x,t)}{\tau_T} \tag{7}$$

where c_i denotes the i^{th} lattice velocity, Δt is the time step, and τ_{mom} and τ_T are relaxation parameter toward the equilibrium distribution f_i and g_i. This particle velocity vectors depends on the lattice arrangements and in the present work D_2Q_9 model as shown Figure 1(c) is used for flow and temperature distribution functions. The discrete particle velocities for D_2Q_9 is given in eq. (8).

$$c_i = \begin{cases} c_o = (0,0) \\ c_i = c(\cos\theta_i,\ \sin\theta_i) \quad \theta_i = (i-1)\dfrac{\pi}{2} \quad \text{for } i = 1,2,3,4 \\ c_i = c\sqrt{2}(\cos\theta_i, \sin\theta_i) \quad \theta_i = (i-5)\dfrac{\pi}{2} + \dfrac{\pi}{4} \quad \text{for } i = 5,6,7,8 \end{cases} \tag{8}$$

The lattice relaxation time τ_{mom} and τ_T are for flow and temperature field respectively. These lattice relaxation times calculated based on kinematic viscosity (υ) and thermal diffusivity (α) are defined as follows:

$$\upsilon = \frac{2\tau_{mom} - 1}{2} c_s^2 \Delta t \tag{9}$$

and

$$\alpha = \frac{2\tau_T - 1}{2} c_s^2 \Delta t \tag{10}$$

The local equilibrium distribution functions can be formulated as

$$f_i^{eq} = W_i \rho \left[1 + 3\frac{u^{eq}.c_i}{c^2} + \frac{9}{2}\left(\frac{u^{eq}.c_i}{c^2}\right)^2 - \frac{3}{2}\frac{u^{2q}}{c^2} \right] \tag{11}$$

$$g_i^{eq} = W_i T \left[1 + 3\frac{u^{eq}.c_i}{c^2} + \frac{9}{2}\left(\frac{u^{eq}.c_i}{c^2}\right)^2 - \frac{3}{2}\frac{u^{2q}}{c^2} \right] \tag{12}$$

here, c is the lattice speed and is defined as $c = \Delta x/\Delta t = \Delta y/\Delta t$ where Δx and Δy are the lattice spacing in X and Y directions and Δt is the lattice time step. The lattice speed is taken as unity for the present study. W_i is the weighting factor for the D_2Q_9 model and the values of W_i are given in eq. (13)

$$W_i = \begin{cases} \frac{4}{9} & i = 0 \\ \frac{1}{9} & i = 1,2,3,4 \\ \frac{1}{36} & i = 5,6,7,8 \end{cases} \tag{13}$$

The distribution functions are solved using the two processes viz., collision and streaming. The localized collision process is followed by the streaming process which distributes the particle from the neighboring lattice points. The macroscopic variables such as density, velocity and temperature are calculated as;

$$\rho(x,t) = \sum_i f_i(x,t) \tag{14a}$$

$$\rho u(x,t) = \sum_i e_i f_i(x,t) \tag{14b}$$

$$T(x,t) = \sum_i g_i(x,t) \tag{14c}$$

and pressure, p is expressed as

$$p(x,t) = c_s^2 \rho(x,t) \tag{15}$$

2.4. Solution procedure

An in-house LBM code is developed in FORTRAN programming language. The two distribution functions for velocity (eq. 6) and temperature (eq. 7) are solved. Macroscopic variables are initiated and equilibrium distribution functions are calculated for both velocity (eq. 11) and temperature (eq. 12). The boundary conditions are implemented. The equilibrium distribution functions calculated for the lattice is propagated to next lattice by collision and streaming processes and the new equilibrium distribution functions are computed. This process is continued until it satisfies the convergence criteria given in eq. (16)

$$\frac{\sum\left[Nu_{avg}(t+\Delta t)-Nu_{avg}(t)\right]}{\sum Nu_{avg}(t)} \le 1.0\times10^{-6} \qquad (16)$$

2.6. Lattice independence study

The lattice independence study is carried out by considering the lattices as tabulated in Table. 1 The average Nusselt number at wall increase by 0.04% by refining the lattice from 750 to 800 and further from 800 to 850 hence we fixed our lattice size as 850 × 85. Similarly for the other Reynolds numbers the lattice independence study established. The LBM model is validated with the experimental results of Ahmad and Hassan[6]. The developing velocity profiles at different axial distance are plotted for microchannel with D_h = 100 mm and Re = 50 are shown in Figure 2. It gives a good agreement with the experimental velocity profiles reported in [6].

Table 1. Lattice independence study for D_h = 100 mm and Re = 5

Sl. no.	(nx × ny)	Nu_{avg}	% difference
1	500 × 50	4.50	0.90
2	550 × 50	4.55	0.76
3	600 × 50	4.58	0.65
4	650 × 50	4.61	0.56
5	700 × 50	4.64	0.48
6	750 × 50	4.66	0.42
7	800 × 50	4.68	0.36
8	850 × 50	4.70	0.32
9	900 × 50	4.71	0.28
10	950 × 50	4.73	0.24

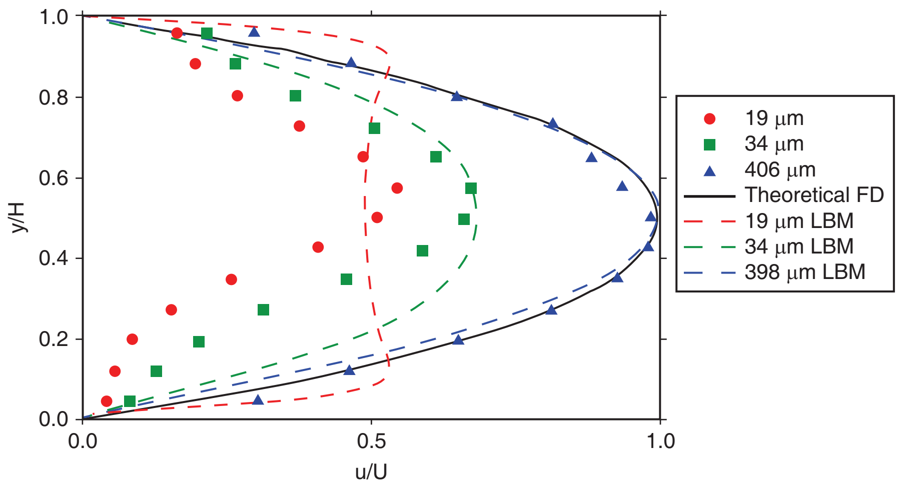

Figure 2. Comparison of developing velocity profiles with Ahmad and Hassan [6] for D_h= 100 mm and Re = 50

3. RESULTS AND DISCUSSIONS

LBM is an useful approach for studying flow and thermal characteristics in microchannel geometries and the present study brings out meaningful information on factors like hydrodynamic and thermal entrance lengths and Nusselt number in microchannel flows using LBM.

Due to the relatively short lengths employed in microchannels, the influence of the entrance region cannot be neglected. The developing velocity profiles at different axial distance from inlet are plotted in Figure 2. The plots are normalized in both the axis. The *Y* axis is normalized distance with respect to the hydraulic diameter of the channel where as the *X* axis shows the normalized velocity with respect to the maximum theoretical fully developed velocity. When flow enters the channel the velocity of the fluid coming in contact with channel wall is immediately reduced to zero (no slip boundary condition). Then consequently the boundary layer develop and propagate towards the centre of the channel. At a certain distance the entire flow field will not vary axially are called to be fully developed flow. The distance at which fluid attain fully developed flow called hydrodynamic entrance length. This entrance length is a function of Reynolds and Prandtl number [13]. The normalized local centerline velocities for different Reynolds numbers are plotted against the non-dimensional axial distance in Figure 3. It is evident from the plot that the centerline velocity remains constant after a certain dimensionless axial distance, and it attain 0.99% of the theoretical fully developed velocity. Apparently we can see the trend

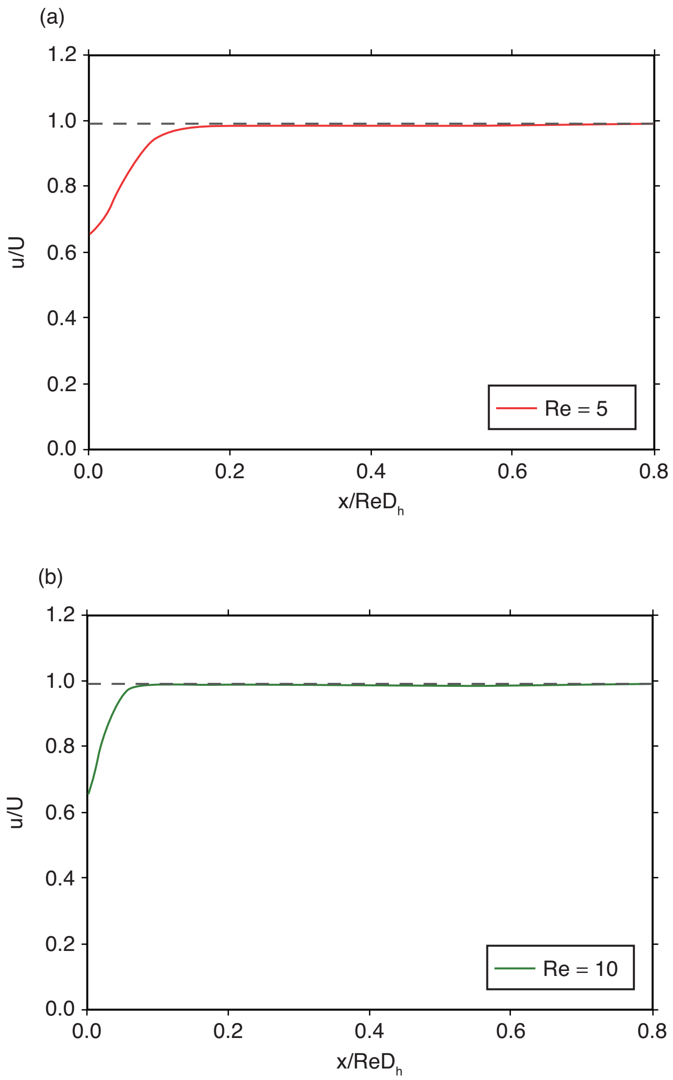

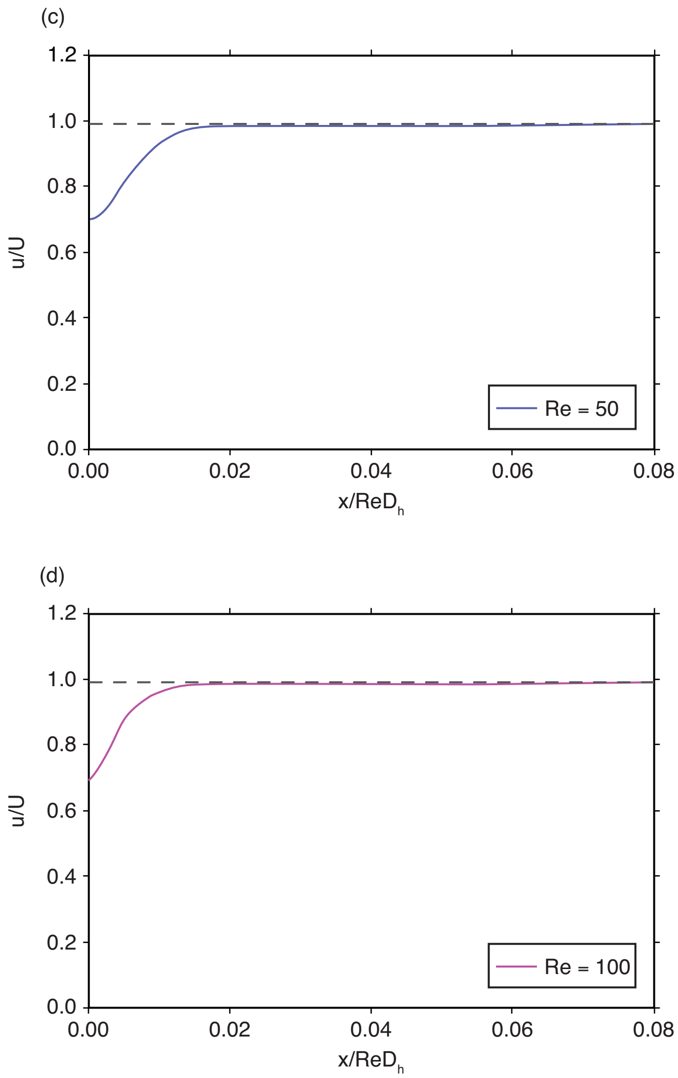

Figure 3. Development of centerline velocity for D_h= 100 mm (a) Re = 5, (b) Re = 10, (c) Re = 50 and (d) Re = 100

is same for all the Reynolds number, and with the increase in Reynolds number the entrance length also increases. The non-dimensional entrance length is plotted in Figure 4 and is found comparable with the correlation as given in eq.(17) proposed by Ahmad and Hassan [6].

$$\frac{L_e}{\mathrm{D_h}} = \left(\frac{0.63}{0.035\,\mathrm{Re}+1}\right) + 0.075\,\mathrm{Re} \tag{17}$$

The thermal entrance length is defined by the axial distance where the non-dimensional bulk mean temperature, $\theta_b = [(T_b - T_i) / (T_w - T_i)]$ is constant. The variation of θ_b with normalized axial distance for different Reynolds numbers is shown in Figure 5. For low Reynolds number cases considered the flow is thermally fully developed within the domain as shown in Figure 5(a) and Figure 5(b) and with the increase in Reynolds number the entrance length also increases. The flow is developing for high

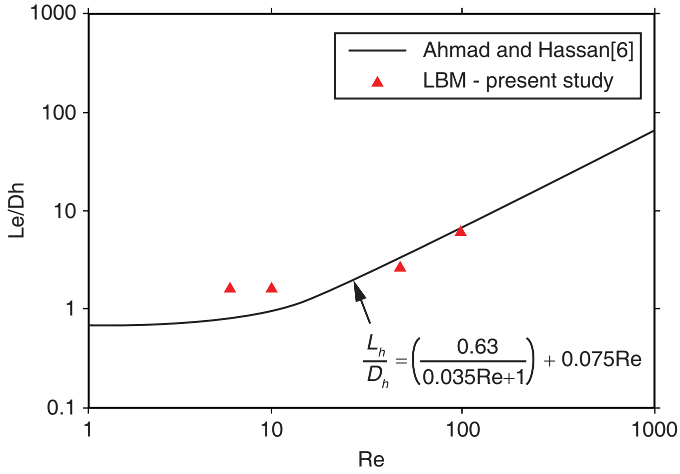

Figure 4. Hydrodynamic entrance length comparison with correlation given by Ahmad and Hassan [6]

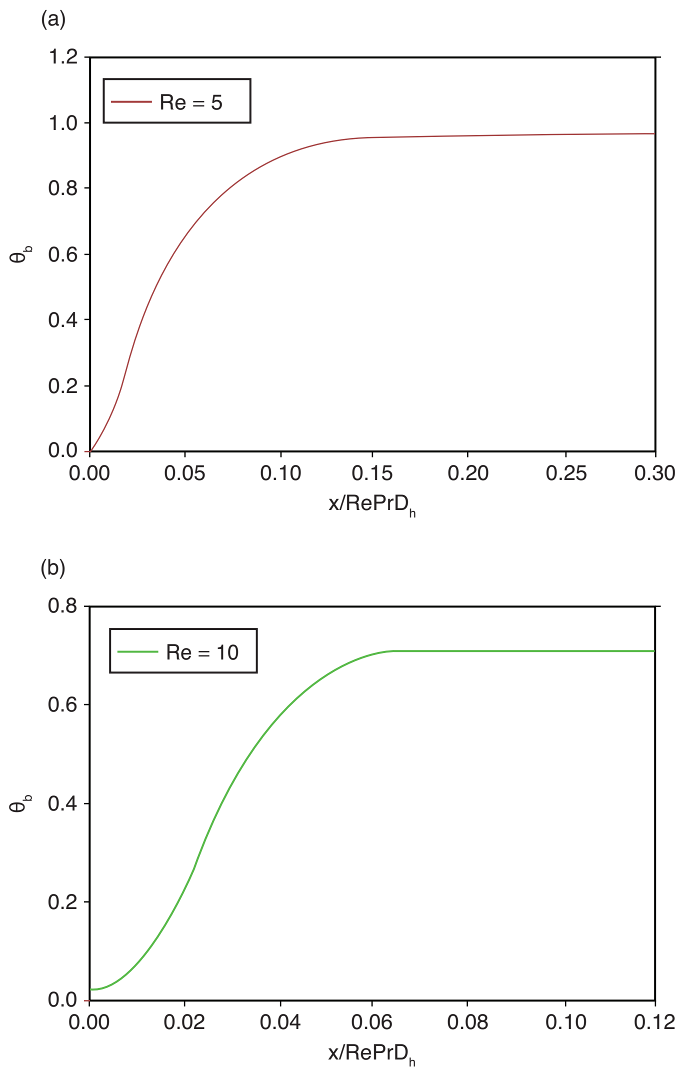

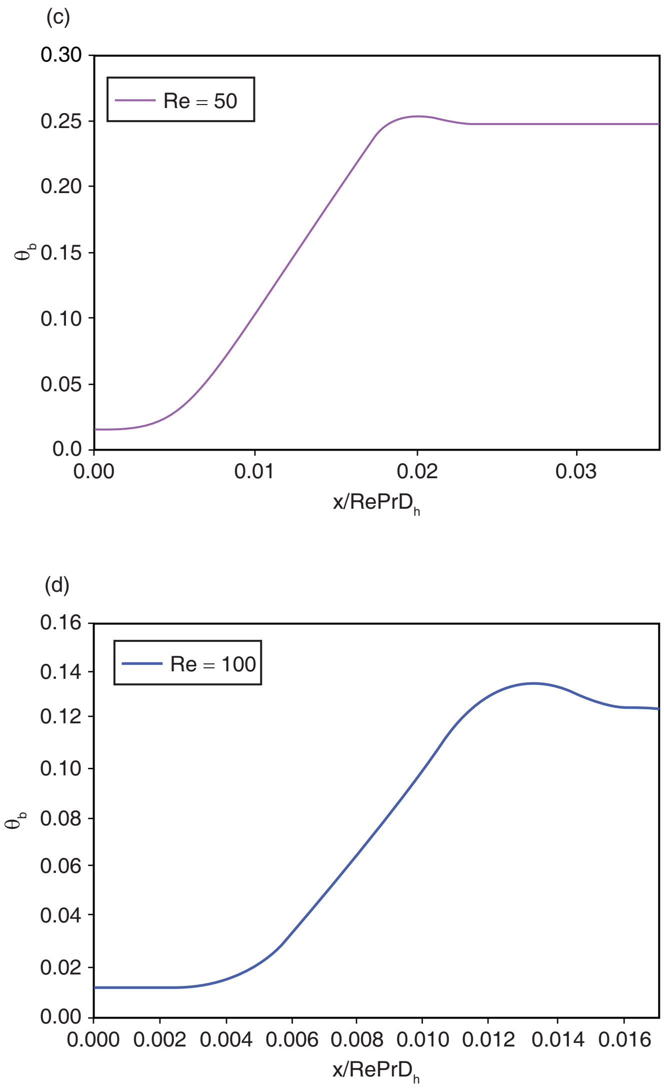

Figure 5. Development of non-dimensional bulk mean temperature with non-dimensional axial distance for D_h= 100mm (a) Re = 5, (b) Re = 10, (c) Re = 50 and (d) Re = 100

Reynolds number as shown in Figure 5(c) and Figure 5(d) in the domain. The Nusselt number increases with Reynolds number is shown in Figure 6 which follow the trend given by Kandlikar *et al*.[14].

4. CONCLUSIONS

The particle based LBM model is successfully applied in the present study to simulate a pressure driven flow in a two-dimensional microchannel. The velocity profiles obtained by the present model compares well with the experimental data in literature. The hydrodynamic entrance length, centerline velocity, thermal entrance length and average Nusselt number are reported for different Reynolds numbers and it is observed that LBM predicts the experimental results quite accurately.

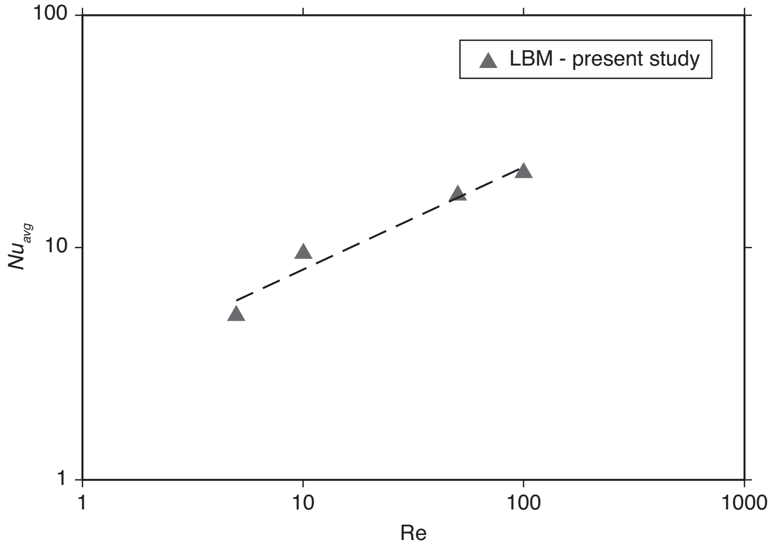

Figure 6. Average Nusselt number variation with Reynolds number

5. ACKNOWLEDGEMENT

The authors would like to acknowledge the computational support provided by the High Performance Computing Facility at Indian Institute of Technology Madras.

6. REFERENCES

[1] Fleming, D. P., and Sparrow, E. M., 1969, *Flow in the hydrodynamic entrance region of ducts of arbitrary cross Section*, Journal of Heat Transfer, 91(3), pp. 345–354.

[2] Atkinson, B., Brocklebank, M. P., Card, C. C. H., and Smith, J. M., 1969, *Low Reynolds number developing Flow,* AIChE Journal, 15(4), pp. 548–553.

[3] Chen, S., and Doolen, G. D., 1998, *Lattice Boltzmann Method for Fluid Flows,* Annual Review of Fluid Mechanics, 30(1), pp. 329–364.

[4] Wibulswas, P., 1966, *Laminar-flow heat-transfer in non-circular ducts,* PhD thesis, University of London.

[5] Aparecido, J., and Cotta, R., 1990, *Thermally developing laminar flow inside rectangular ducts,* International Journal of Heat and Mass Transfer, 33(2), pp. 341–347.

[6] Ahmad, T., and Hassan, I., 2010, *Experimental analysis of microchannel entrance length characteristics using microparticle image velocimetry*, Journal of Fluids Engineering, 132(4), pp. 041102–041102.

[7] Lee, P.S., and Garimella, S. V., 2006, *Thermally developing flow and heat transfer in rectangular microchannels of different aspect ratios*, International Journal of Heat and Mass Transfer, 49(17), pp. 3060–3067.

[8] Mohamad, A. A., 2011, *Lattice Boltzmann method: fundamentals and engineering applications with computer codes,* Springer.

[9] Lim, C., Shu, C., Niu, X., and Chew, Y., 2002, *Application of lattice boltzmann method to simulate microchannel Flows*, Physics of Fluids, 14(7), pp. 2299–2308.

[10] Nie, X., Doolen, G. D., and Chen, S., 2002, *Lattice Boltzmann simulations of fluid flows in MEMS*, Journal of Statistical Physics, 107(1-2), pp. 279–289.

[11] Niu, X., Shu, C., and Chew, Y., 2004, *A lattice boltzmann BGK model for simulation of micro flows*, Europhysics Letters, 67(4), p. 600.

[12] Zhou, Y., Zhang, R., Staroselsky, I., and Chen, H., 2004, *Numerical simulation of laminar and turbulent buoyancy-driven flows using a lattice boltzmann based algorithm*, International Journal of Heat and Mass Transfer, 47(22), pp. 4869–4879.

[13] Sparrow, E., Lin, S., and Lundgren, T., 1964, *Flow development in the hydrodynamic entrance region of tubes and Ducts*, Physics of Fluids, 7, p. 338.

[14] Kandlikar, S., Garimella, S., Li, D., Colin, S., and King, M. R., 2005, *Heat transfer and fluid flow in minichannels and Microchannels*, Elsevier.